Density log correction for borehole effects and its impact on well-to-seismic tie: Application on a North Sea data set

Isadora A. S. de Macedo[1], Jose Jadsom S. de Figueiredo[1], and Matias C. de Sousa[1]

Abstract

Reservoir characterization requires accurate elastic logs. It is necessary to guarantee that the logging tool is stable during the drilling process to avoid compromising the measurements of the physical properties in the formation in the vicinity of the well. Irregularities along the borehole may happen, especially if the drilling device is passing through unconsolidated formations. This affects the signals recorded by the logging tool, and the measurements may be more impacted by the drilling mud than by the formation. The caliper log indicates the change in the diameter of the borehole with depth and can be used as an indicator of the quality of other logs whose data have been degraded by the enlargement or shrinkage of the borehole wall. Damaged well-log data, particularly density and velocity profiles, affect the quality and accuracy of the well-to-seismic tie. To investigate the effects of borehole enlargement on the well-to-seismic tie, an analysis of density log correction was performed. This approach uses Doll's geometric factor to correct the density log for wellbore enlargement using the caliper readings. Because the wavelet is an important factor on the well tie, we tested our methodology with statistical and deterministic wavelet estimations. For both cases, the results using the real data set from the Viking Graben field — North Sea indicated up to a 7% improvement on the correlation between the real and synthetic seismic traces for well-to-seismic tie when the density correction was made.

Introduction

The well-to-seismic tie is an important tool in seismic inversion and interpretation. It can join the vertical resolution of the well logs with the horizontal resolution of the seismic data, thus enabling the identification of stratigraphic markers on the seismic section and the correct estimate of the wavelet. Consequently, with the proper wavelet, the real seismic data can be inverted to reflectivity or impedance. In general, the basic principle behind a well tie is to compute a synthetic seismic trace and compare it with the real seismic trace. The convolutional model is the basis for most well tie procedures because it establishes a relationship between the reflectivity function calculated from the well-log data, the seismic wavelet, and the synthetic seismic trace. According to White and Simm (2003), the methods to estimate the seismic wavelet are divided into two categories: deterministic and statistical. The deterministic method requires direct measurements of the source wavefield or the use of the well-log data (Oldenburg et al., 1981; Yilmaz, 2000). Statistical methods estimate the wavelet from the seismic trace itself, and depending on the approach used, they require assumptions about the characteristics of the wavelet (Buland and Omre, 2003; Lundsgaard et al., 2015), such as the requirement of minimum phase. The main factors controlling the accuracy of the well-to-seismic tie are the seismic wavelet, a coherent time-depth relationship, and the accuracy of the elastic well-log data. The time-depth relationship is used to generate a reflectivity series in the time domain. Accurate elastic well-log data produce a reliable reflectivity series in depth.

An accurate well tie for the characterization of any reservoir requires accurate elastic logs. The comprehensive information provided by wireline procedures, when tied properly to land seismic data, allows interpreters to verify whether their geologic conclusions about the seismic background are suitable to the observed lithologic parameters (White and Hu, 1998). A central matter to the well profile interpretation are the log corrections, which can be challenging (Serra, 1994). The change in well diameter along the drilling is a factor that can affect the measurements made by the tool; therefore, corrections must be applied to preserve the meaning of the log values (Ellis and Singer, 2007). Although the stability of the wellbore is controlled during the drilling process, nonpredicted occurrences of formation collapse change the distribution of the physical properties around the wellbore. The consequence are anomalous values observed in the

[1]Federal University of Pará (UFPA), Faculty of Geophysics, Faculty of Geophysics, Petrophysics and Rock Physics Laboratory - Prof. Dr. Om Prakash Verma, Belém, Par´, Brazil. E-mail: isadora.s.macedo@gmail.com; jadsomjose@gmail.com; matiasdsousa@gmail.com.

Manuscript received by the Editor 8 January 2019; revised manuscript received 23 August 2019; published ahead of production 07 October 2020. This paper appears in *Interpretation*, Vol. 8, No. 1 (February 2020); p. 1–11, 9 FIGS.

http://dx.doi.org/10.1190/INT-2019-0004.1.

caliper log in the regions where the formation collapse occurred.

Borehole enlargement implies log distortions, including incorrect density measurements that result from mixing the formation components with the drilling mud (Liu and Zhao, 2015). This interaction of the drilling fluid and the formations around the wellbore is a relevant factor to be concerned for in-depth acquisitions, especially regarding the density log, whose precision is directly related to the well-to-seismic tie response. In a situation in which the mud density is lower than the formation bulk density, an expanded borehole or an irregular wellbore wall affect the density log curve so markedly that the curve drops precipitously, and the measured density value is much lower than the true density value (Yong and Zhang, 2007). On the other hand, in cases in which the mud density is greater than the formation bulk density, the opposite happens: The density curve would increase rather than drop, and the apparent density would be greater than the formation bulk density.

Macedo et al. (2017) analyze the influence of the stability of the borehole diameter during acquisition on the well-to-seismic tie and show that anomalies on the caliper logs can directly affect the quality of the tie and, consequently, the estimated wavelet. Within this scenario, the present paper aims to analyze the well-to-seismic tie response when the proper corrections on the density log for the wellbore enlargement are made. These corrections are based on Doll's geometric factor. To verify the feasibility of our proposed methodology, we perform well-to-seismic tie on the real data set from the Viking Graben field — the North Sea with and without density log correction — and with two different wavelet estimation methods: a classical deterministic approach and a statistical approach through the predictive deconvolution.

Theory

Well-to-seismic tie procedure

The well-to-seismic tie procedure requires the forward modeling of the synthetic seismic trace. It is performed by the convolution of the reflectivity series created directly from the sonic log and bulk density curves with the seismic wavelet. The synthetic seismogram is constructed through the following equation:

$$s(t) = w(t) * r(t), \tag{1}$$

where $s(t)$ represents the synthetic seismic trace, $w(t)$ represents the seismic wavelet, and $r(t)$ is the reflectivity converted to the time domain. Before converting the reflectivity series to the time domain, one must calculate it in depth from the density and velocity logs. Mathematically, the discretized reflectivity R_c in depth is represented by

$$R_c(i) = \frac{\rho_{b_{i+1}} v_{i+1} - \rho_{b_i} v_i}{\rho_{b_{i+1}} v_{i+1} + \rho_{b_i} v_i}, \tag{2}$$

where i represents the index of a sample in depth, R_c is the reflectivity in the depth domain, v is the P-wave velocity, and ρ_b is the bulk density. The reflectivity, calculated in-depth, needs to be placed in the time domain by the proper establishment of the time-depth relationship, which can be achieved by check-shot surveys or vertical seismic profile (VSP) data.

Correlation is a measure of coherence that can be used to compare the real and synthetic seismic traces for well tie purposes. Correlations between variables can be measured with the use of different indices (coefficients). The three most popular are Pearson's coefficient, Spearman's coefficient, and Kendall's tau coefficient (Hauke and Kossowski, 2011). The choice of each correlation coefficient depends on the type of data being analyzed. Spearman's and Kendall's correlation coefficients are used for interval or ordinal data. The Pearson correlation coefficient, the one used in this work, is appropriate only for interval data (Chok, 2010).

The Pearson correlation coefficient (r) measures the strength and direction of the linear relationship between two independent variables, giving a sense of the degree to which one variable is linearly related to another. Its values lie between ± 1 and are calculated according to the following equation:

$$r = \frac{\sum_{i=1}^{N}(x_i - \bar{x})(y_i - \bar{y})}{\sqrt{\sum_{i=1}^{N}(x_i - \bar{x})^2}\sqrt{\sum_{i=1}^{N}(y_i - \bar{y})^2}}, \tag{3}$$

where N is the total number of samples, i is the index of samples, and $\bar{x}, \bar{y}$ are the means. For the case of the well-to-seismic tie, vector $\mathbf{x}$ represents the real seismic trace, whereas vector $\mathbf{y}$ represents the synthetic seismic trace.

Density log measurements

The bulk density curve is crucial for calculation of reflectivity. The density estimated by the logging tool is based on back-scattering (from Compton scattering) gamma radiation emitted by a radioactive source such as Cs^{137} or Co^{60}. The gamma rays emitted from a source will interact with the electrons of the formation. The higher the electron density of the formation, the higher is the number of collisions of the gamma rays with the electrons and, consequently, the lower is the intensity of gamma-rays detected by the sensor. The intensity of gamma rays detected is expressed by

$$I = I_o e^{-\mu \rho_e L}, \tag{4}$$

where I is the intensity of gamma rays detected by the scintillometer, I_o is the intensity of gamma rays at the source, μ is a constant that depends on the geometry of the tool, ρ_e is the density of electrons of the formation, and L is the distance between the source and the detector. The electron density ρ_e and the bulk density ρ_b of the formation are related through the following equation:

$$\rho_e = \rho_b \frac{Z}{A} N, \tag{5}$$

where Z is the atomic number, A is the atomic mass, and N is the Avogadro number (6.023×10^{23}). Because for most of the formations ($Z/A \approx 1/2$), equation 5 becomes

$$\rho_e = \rho_b \frac{N}{2}. \tag{6}$$

By substituting equation 6 into equation 4, the intensity of detected gamma rays becomes

$$I = I_o e^{-\mu \frac{\rho_b N}{2} L}. \tag{7}$$

Taking the logarithm of both sides of equation 7, we have the density of formation ρ_b in terms of the intensity of the gamma ray detected by the sensor in the logging tool:

$$\rho_b = \frac{2[LnI_o - LnI]}{\mu N L}. \tag{8}$$

The lower the source-detector distance, the lower is the depth of investigation, which makes the density formation values more influenced by the borehole enlargement. Moreover, the depth of investigation also decreases with the increase in the density of the formation.

The first single-detector density tool measurements suffered from the effects of mud-cake and were marketed in the mid-1950s (Labo, 1987; Serra, 1994). The second-generation tool uses a two-detector system that compensates for near-borehole problems (Labo, 1987). According to Serra (1994), the effect of the borehole is more severe for uncompensated density logs but less so for the compensated ones. The author also states that if the borehole wall is not smooth, the formation density compensated pad is not correctly applied to the formation and isolates zones full of mud, which strongly affect the measurement. Therefore, even if the tool has a compensation system to mitigate the effect of the rugosity of the borehole wall, if the borehole enlargement is severe, it will still affect the density log values. It can be assumed that the medium where the density logging tool operates is composed of rock formations and drilling mud. The density measured by the tool is therefore derived from the formation density and the drilling mud density. The traditional correction schemes for density has some limitations because beyond some mudcake thickness (≈1in), depending on the tool design details that control, in part, the depth of investigation, the compensation scheme breaks down, and the estimate of the bulk density will be in doubt (Ellis and Singer, 2007). According to Ellis and Singer (2007), the auxiliary measurement that is most helpful to indicate suspicious density readings is the caliper. Motivated by those reasons, Doll's geometric factor was used as an attempt to correct the density log for the effects of severe borehole enlargement along with the use of the caliper readings.

Methodology

Correcting the density log for the borehole enlargement

To correct the density log for the borehole enlargement through the caliper log readings, we used Doll's geometric factor. Doll (1949) develops the apparent geometric factor theory for the induction logging, which was created to measure formation resistivity in boreholes containing oil-based muds and in air-drilled boreholes because electrode devices could not work in these nonconductive boreholes. For the induction logging, the theory states that the voltage at the receiver is the sum of the contribution of a large number of infinitesimal rings of the Foucault current. The geometric factor of each coaxial cylindrical area would represent the fraction of contribution of this single area to the entire signal, assuming a uniform conductivity within each zone.

The presence of unconsolidated formations compromises the signals recorded by the logging tool. When the formation in the vicinity of the well is homogeneous and there are no washout zones, the density measured by the logging tool is similar to the correct density of the formation. However, when the formation is heterogeneous, the apparent density measured by the tool represents a combination of the densities of the different formations that exist around the well. The influence of each formation can be considered separately, and the signal measured is represented by the sum of each signal generated by each formation.

To properly use the apparent geometric factor theory for the density logging, it is necessary to establish the geometry of the borehole environment we are assuming in our methodology. The following assumptions are made: (1) different zones around the well are concentric and, therefore, have a rotation symmetry, (2) the geometry of the borehole is a cylinder of radius similar to the drill bit, and (3) the diameter of the borehole maintained its size during the drilling procedure.

The vicinity of the well is composed of the rock formation and the drilling mud. As proposed by Doll (1949) for induction logging, the density measurement can also be obtained from a weighted average of mud and formation densities in equation 10 as a consequence of the apparent geometric factor that satisfies the condition

$$G_b + G_{\text{mud}} = 1, \tag{9}$$

and

$$\rho_a = G_b \rho_b + G_{\text{mud}} \rho_{\text{mud}}, \tag{10}$$

where G_b is the coefficient for the formation rock, $0 \le G_b \le 1$; G_{mud} is the coefficient for the mud, $0 \le G_{\text{mud}} \le 1$; ρ_a is the apparent density (g/cm^3); ρ_b

is the bulk density (g/cm^3); and ρ_{mud} is the mud density (g/cm^3). If there is significant borehole diameter expansion, all values are represented by the mud density. According to equations 9 and 10, $G_{mud} = 1$, $G_b = 0$, $\rho_a = \rho_{mud}$; in contrast, if the logging tool keeps contact with a regular wellbore wall, then $G_{mud} = 0$, $G_b = 1$, $\rho_a = \rho_b$. Therefore, in terms of error estimation due to borehole expansion, G_{mud} and ρ_{mud} are the fundamental parameters that needed to be investigated.

To determine the true values of density that represent the subsurface formations, we derive from equations 9 and 10 the following expression:

$$\rho_b = \frac{\rho_a - G_{mud}\rho_{mud}}{1 - G_{mud}}, \tag{11}$$

which indicates the corrected value of bulk density, in terms of apparent density, mud density, and apparent geometry factor of mud. The method we used to analyze how the borehole effect affects the well-to-seismic tie results consists of search for a value for G_{mud} and ρ_{mud} using equation 11 to investigate the proper values of formation density (ρ_b).

We performed the correction on the density log at each point in depth by creating a linear relationship between the minimum and maximum values of the caliper log with the minimum and maximum values of the apparent geometric factor of the mud G_{mud}. From equation 10, one can note that when $G_{mud} = 0$, the corrected bulk density is equal to the measured bulk density. The choice of the maximum value of G_{mud}, related to the maximum value of the caliper log, must be based on the depth of investigation of the density logging tool. To create a log of G_{mud} values in-depth to proceed with the correction of the bulk density log at each point in depth, a linear relationship between the caliper log and the G_{mud} values was established according to the equations described below and the graphic from Figure 1.

As the diameter of the borehole increases, the density log value decreases; on the contrary, density log values increase as borehole diameters approach normal

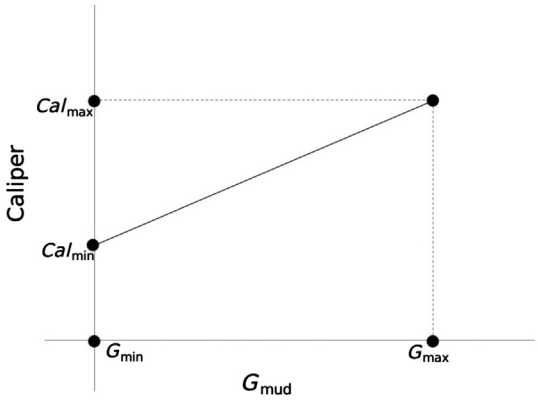

Figure 1. The linear relationship between the apparent geometric factor G_{mud} and the caliper log, according to its maximum and minimum values.

levels. This means that on the portions of the density log where the enlargement of the borehole occurs, the density log values are underestimated. Hence, the correction for the geometry of the wellbore should increase the values of the density log on those portions. To correct the density log for the geometry of the borehole, we calculate the slope and intercept of the line of Figure 1:

$$m = \frac{\mathrm{Cal}_{max} - \mathrm{Cal}_{min}}{G_{max} - G_{min}}, \tag{12}$$

and

$$b = \mathrm{Cal}_{min} - mG_{min}, \tag{13}$$

where Cal_{max} and Cal_{min} represents the maximum and minimum value of the caliper log, and G_{max} and G_{min} represents the maximum and minimum value of the apparent geometric factor of the mud G_{mud}, with the minimum value being zero and the maximum value depending upon the geology and the logging tool. For the Viking Graben dataset (the real data used in this paper), we set $G_{max} = 0.4$.

Accordingly, the G_{mud} log is created through the equation

$$G_{mud} = \frac{\mathrm{Cal} - \mathrm{Cal}_{min}}{m} + G_{min}, \tag{14}$$

where Cal represents each value of the caliper log in depth and G_{mud} is each value of G_{mud} created along the depth axis. By applying the relation 14 in equation 11, we generate the relation that we used to correct the bulk density value for each point in depth 15:

$$\rho_b = \frac{\rho_a - [(\mathrm{Cal} - \mathrm{Cal}_{min})/m + G_{min}]\rho_{mud}}{1 - [(\mathrm{Cal} - \mathrm{Cal}_{min})/m + G_{min}]}. \tag{15}$$

In the situation where there is no enlargement of the borehole (when the caliper log is stable), $m = 0$ and equation 15 becomes

$$\rho_b = \frac{\rho_a - G_{min}\rho_{mud}}{[1 - G_{min}]}. \tag{16}$$

Also, in this situation, the minimum value of the apparent geometric factor of the mud is $G_{min} = 0$. Hence, when the caliper log is stable and the diameter of the borehole maintains its bit size during the drilling, there is no need to correct the measured bulk density because $\rho_b = \rho_a$. The procedure to perform the correction on the density log is shown in the flowchart of Figure 2, and the complete procedure to perform the correction and the well-to-seismic tie are described in the following steps and in charts in Figures 2 and 3:

1) Edit the sonic and density logs to remove noisy spikes.
2) Establish the range of possible values of ρ_{mud}.

3) Establish the value of G_{max} and set $G_{min} = 0$.
4) Create the G_{mud} log in depth according to equation 14.
5) Perform the correction on the measured density log using the G_{mud} log and equation 15.
6) Calculate the reflectivity series with the corrected density log using equation 2.
7) Estimate the seismic wavelets through the deterministic and statistical approaches.
8) Convolve the reflectivity series with the estimated wavelets to calculate the synthetic seismic trace.
9) Compare the synthetic seismic trace with the real seismic trace through cross-correlation.
10) Compare the correlation of the well-to-seismic tie without correction on the density log with the correlation of the well-to-seismic tie with the correction on the density log.

Estimation of the wavelet

The estimation of the wavelet is a key feature of the well-to-seismic tie. Deterministic methods to estimate the wavelet uses seismic and well-log data. The deterministic methods based on the Wiener filtering technique, for instance, are based on the classic assumptions of the convolutional model, in which the limiting factors are the premises of a random process reflectivity and a minimum-phase wavelet. Deterministic methods based on least-squares minimization circumvent these objections. Statistical methods to estimate the wavelet use only the seismic data. One possible approach is through the predictive deconvolution, which also implies the assumption of a random process reflectivity and a minimum-phase wavelet. It is possible to perform a statistical estimate of the wavelet without these limitations, by using, for example, the homomorphic deconvolution. To maintain both estimates of the wavelet under the same premises, we used a deterministic and a statistical estimation based on the classical assumptions of the convolutional model. By fixing it, it is possible to analyze the well-tie response only due to the effect of the correction on the density log for the borehole enlargement and analyze its behavior according to the two general techniques to estimate the wavelet.

The wavelets in this study were estimated by two different approaches: a statistic estimation through predictive deconvolution using the optimum Wiener filter, and a deterministic extraction by building a filter, using the seismic trace and well-log data. To study the influence of the corrected density log, we used the same wavelet for the well ties with and without correction on the density log. For the traditional deterministic wavelet estimation, different wavelets are extracted when different density logs are generated. The results of the application of the predictive deconvolution to estimate the wavelet were also used by Macedo et al. (2017).

The predictive deconvolution is a special case of the Wiener filtering, which requires the solution of the normal equations:

$$\begin{pmatrix} r_0 & r_1 & r_2 & \cdots & r_{n-1} \\ r_1 & r_0 & r_1 & \cdots & r_{n-2} \\ r_2 & r_1 & r_0 & \cdots & r_{n-3} \\ \vdots & \vdots & \vdots & \ddots & \vdots \\ r_{n-1} & r_{n-2} & r_{n-3} & \cdots & r_0 \end{pmatrix} \begin{pmatrix} a_0 \\ a_1 \\ a_2 \\ \vdots \\ a_{n-1} \end{pmatrix} = \begin{pmatrix} g_0 \\ g_1 \\ g_2 \\ \vdots \\ g_{n-1} \end{pmatrix}, \tag{17}$$

where r_i represents the autocorrelation lags of the input wavelet, a_i is the Wiener filter coefficients, and g_i are the crosscorrelations lags of the desired output with the input wavelet. The prediction process is assumed when the desired output on the normal equations is a time-advanced form of the input series. In the case of the predictive deconvolution, given an input series

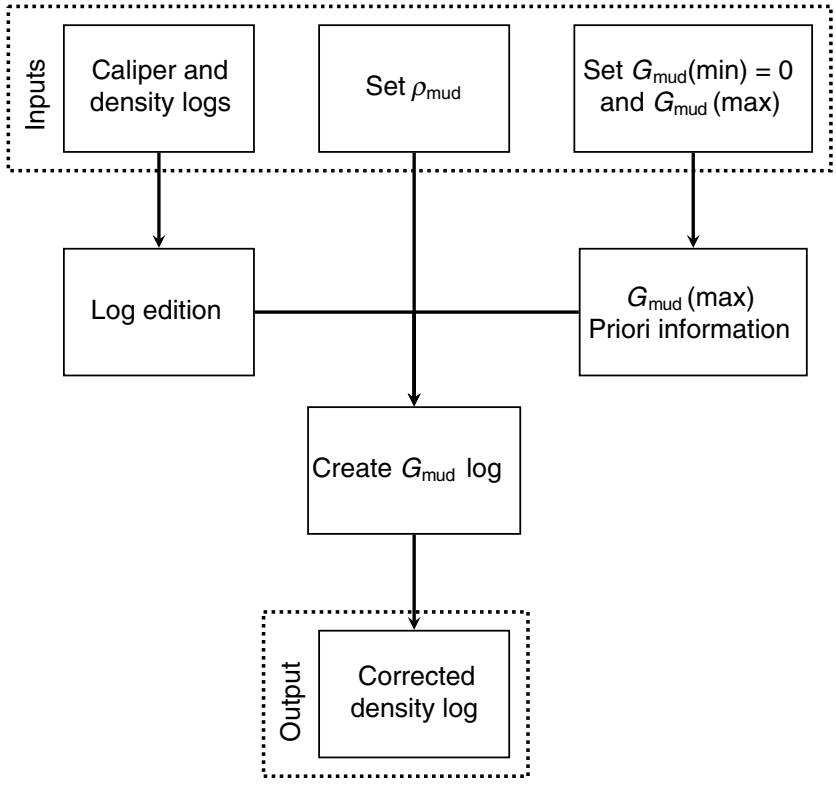

Figure 2. The flow diagram indicating the procedure to correct the density log for the borehole enlargement. The first steps are the log editions for despiking, and to remove null values, set a usual value for the ρ_{mud}, set the minimum value of G_{mud} as zero, and set the maximum value of G_{mud} according to the prior information and depth of investigation of the tool. With this information, it is possible to create the G_{mud} log that will be used to correct the density log for the borehole enlargement for each point in depth.

$x(t)$, the goal is to predict its value at some posterior time $x(t+\alpha)$, where α is the prediction lag. Using the normal Wiener equations to build a filter to estimate $x(t+\alpha)$ (the new desire output that must be cross-correlated with the input $x(t)$), it gives

$$\begin{pmatrix} r_0 & r_1 & r_2 & \cdots & r_{n-1} \\ r_1 & r_0 & r_1 & \cdots & r_{n-2} \\ r_2 & r_1 & r_0 & \cdots & r_{n-3} \\ \vdots & \vdots & \vdots & \ddots & \vdots \\ r_{n-1} & r_{n-2} & r_{n-3} & \cdots & r_0 \end{pmatrix} \begin{pmatrix} a_0 \\ a_1 \\ a_2 \\ \vdots \\ a_{n-1} \end{pmatrix} = \begin{pmatrix} r_\alpha \\ r_{\alpha+1} \\ r_{\alpha+2} \\ \vdots \\ r_{\alpha+n-1} \end{pmatrix}. \tag{18}$$

That is the case for an n-long prediction filter and an α-long prediction lag. The prediction filter requires only the autocorrelation of the input series, which configures a statistical estimation of the wavelet. According to Robinson and Treitel (2008), the canonical representation of the seismic trace is the convolution of an all-pass filter — with a flat magnitude spectrum — and a minimum-delay wavelet. The trace and the wavelet have the same nonflat magnitude spectrum. The predictive deconvolution separates the components of the trace on the basis of the criteria of minimum-delay and white: The error series of the predictive deconvolution yields the white components of the seismic trace (all-pass filter and the reflectivity), and the prediction filter yields the predictable components of the seismic trace, which is the minimum-delay component that constitutes the minimum-phase estimated wavelet.

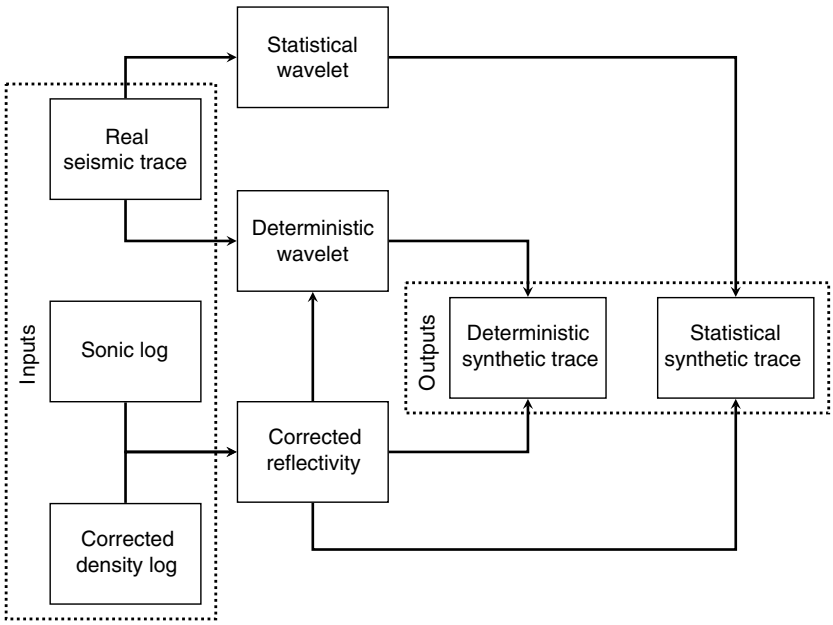

Figure 3. The flow diagram indicating the procedure to perform the well-to-seismic tie after the correction on density log. The corrected reflectivity is calculated, and two wavelets are estimated: a statistical wavelet through the predictive deconvolution, which uses only the real seismic trace; a deterministic wavelet, from the corrected reflectivity and the real seismic trace. The convolution of those wavelets with the corrected reflectivity will produce the statistical synthetic trace and the deterministic synthetic trace, respectively.

Therefore, we selected a segment of the trace that we believed to be a result of a reflector and deconvolved that segment to separate the white components from the minimum-phase component, by choosing a prediction lag and operator length. For a single segment in time of the real seismic trace, we selected a range of prediction lag and a range of operator length and performed the deconvolution to estimate the wavelet. The algorithm returns the prediction lag and operator length that produces the best wavelet that matches the synthetic trace and the real trace.

The deterministic extraction of the wavelet is made by the building of a filter that when convolved with the reflectivity produces the best match between the synthetic trace (provided by the convolution of the filter coefficients and the reflectivity), with the real seismic trace. The inputs to the deterministic wavelet extraction are the reflectivity series, the seismic trace, the length of the filter (wavelet), and the increment in time, which corresponds to the best shift between the reflectivity series and the real seismic trace. For a given range of length of filter and increment, the algorithm returns the best parameters that produce the wavelet that best matches the synthetic trace and the real seismic trace.

Results on the Viking Graben data set

Geologic background

The Viking Graben is located in the North Sea Basin, and it is the product of a rifting event during the late Permian to the Triassic. The formation of the oil and gas of the North Sea is related to an extensional episode at the beginning of Jurassic, which caused Pangea to break into the continents Gondwana and Laurasia. Details regarding the stratigraphy of the Viking Graben can be found in Madiba and McMechan (2003), Keys and Foster (1998), and Macedo et al. (2017). The data set used in this study was the subject of a 1994 SEG workshop on comparison of seismic inversion methods (Keys and Foster, 1998). The seismic data consist of a 2D seismic line, oriented east–west, with 2142 CMPs separated by 12.5 m, each CMP with 1501 samples and a sample rate of 0.004 s. The well-log information is from two wells named well A and well B. Macedo et al. (2017) perform well-tie procedures using these logs and the same seismic section, verifying that the best match to the well data is the CMP 809 for well A, which we also used as a real seismic trace. The well logs were edited to remove noisy spikes and null values.

Numerical experiments and discussion

In this section, we present our results of the well-to-seismic tie applied on the Viking Graben data set with the correction on the density log for the borehole enlargement. We used two different ways to estimate the seismic wavelet: the deterministic approach and the statistical approach, through the predictive deconvolution (Macedo et al., 2017). For the deterministic seismic wavelet estimation, we performed the correction on the density log in two ways: The first is correcting the entire density log, and the second is performing the correction only on the segments of the density log where the corresponding caliper log is unstable. We did that because the deterministic wavelet estimation is dependent on the reflectivity series. Therefore, different corrections produce different reflectivity series and, therefore, produce different deterministic estimated wavelets. It was important to verify when the correction is most effective for the well tie: whether a correction to the entire density log or only in anomalous caliper segments. The statistical wavelet estimation is dependent only on the seismic wavelet; therefore, different types of corrections on the density log will not change the wavelet estimation — only the reflectivity series to be used on the tie, which does not have a meaningful impact (less than 1%) on the final correlation between the synthetic seismic trace and the real seismic trace.

Figure 4 shows the well logs from the real data set from the Viking Graben field used for the well-to-seismic tie. The despiking procedure was applied to remove the noise spikes. Figure 5 shows the caliper readings, the original and corrected density log, and the correction applied on the original density log, which was produced through our methodology using Doll's geometric factor.

We test different values for the maximum value of G_{mud} and set the maximum value of G_{mud} in 0.4 for this case. By establishing that, the G_{mud} values will range from 0 to 0.4; consequently, the G_b values will range from 0.6 to 1. The value of the geometric factor is related to the depth of investigation of the logging tool. In the case of the density tool, the depth of investigation is small due to the short penetration of the gamma ray into the formation. According to Ellis and Singer (2007), 90% of the response of the density logging tool is influenced by the first 4 in of depth of investigation, which means that there is a strong sensitivity of the tool to the near-borehole zone presumed to be invaded by the drilling mud. Because of that, it is necessary to add more weight to the zones farther from the borehole, where the true value of density could be measured, to obtain a proper measure. Thus, the geometric factor of the formation G_b will vary from 0.6 to 1. These weights are always higher than the established mud weights, which configures an approach to compensate for the higher sensibility of the density tool to the near-borehole zone. Moreover, by establishing those weights, we ensure that the corrected density log maintain its geologic consistency: The fixed density log measurements are not underestimated nor overestimated.

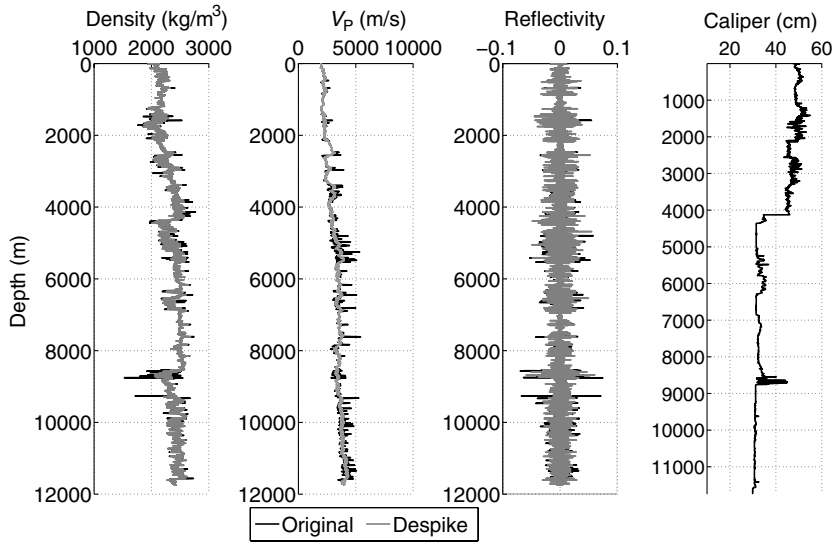

Figure 4. Real well-log data from the Viking Graben field used on the well-to-seismic tie without the proper corrections on the density log and only with the despiking to remove the noisy spikes.

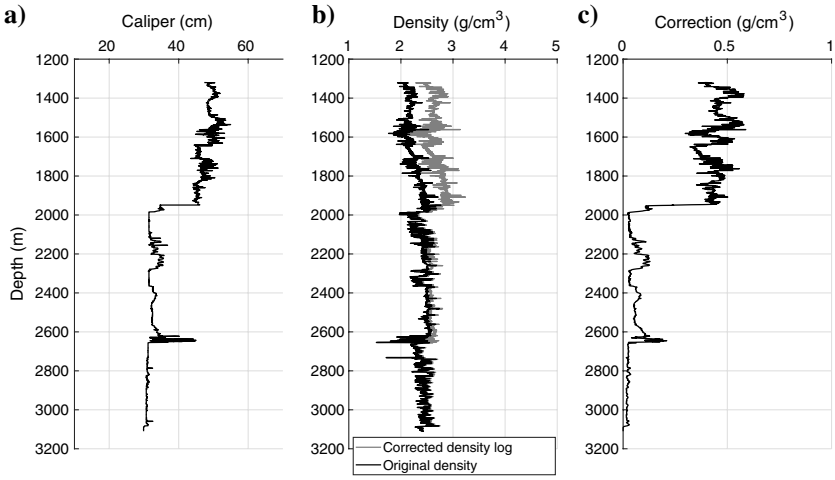

Figure 5. (a) Caliper log used to calculated the correction to be applied on the density log. (b) Original and corrected density log for the borehole enlargement. (c) The calculated correction applied to the original density log.

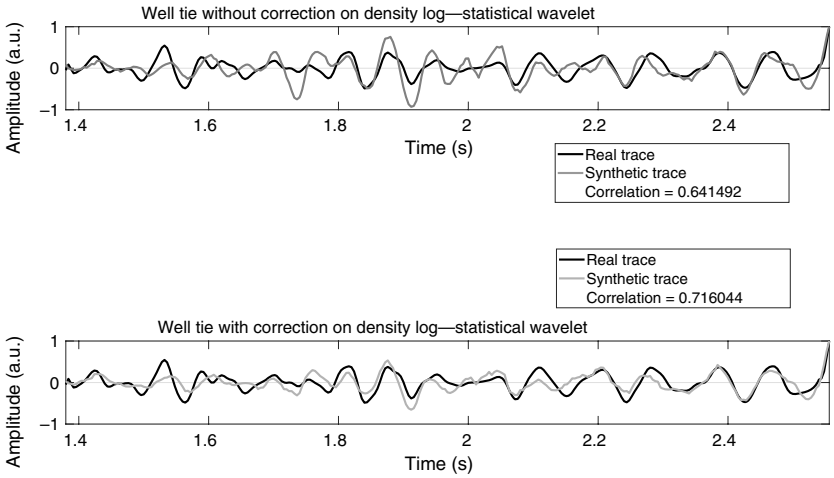

Figure 6. Well-to-seismic tie using a statistical wavelet estimation and a correction on the density log only where the caliper indicates a severe borehole enlargement. The correlation improved from 0.64 to 0.71 when performing the correction.

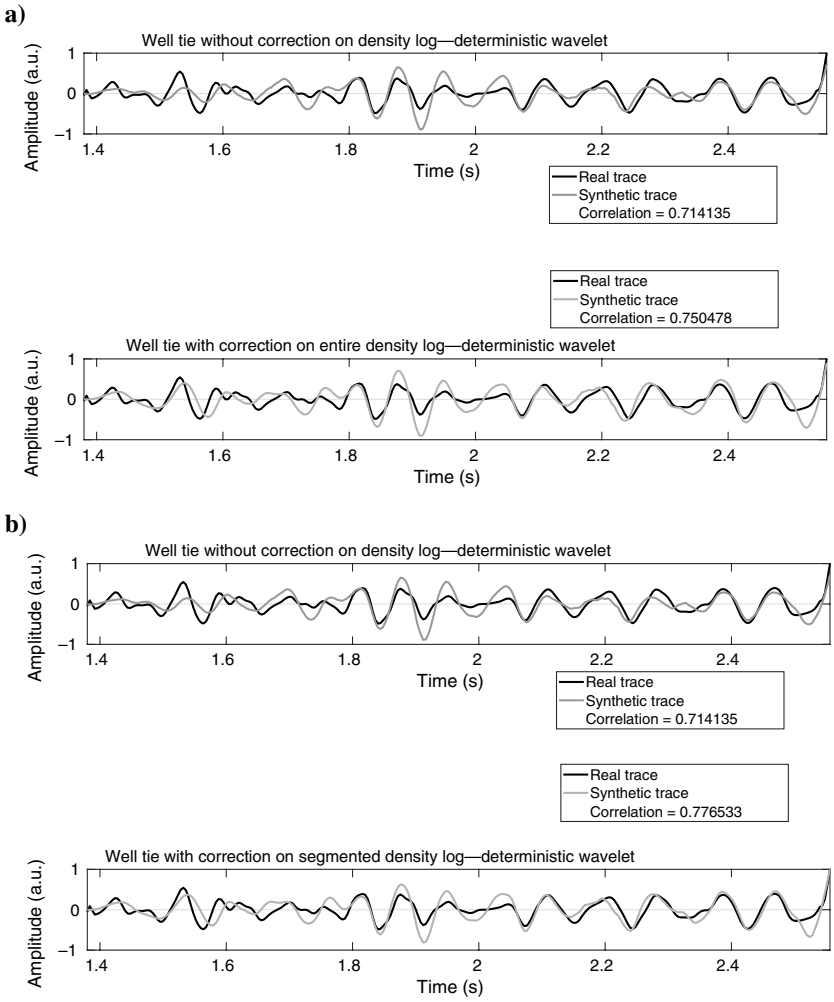

Figure 7. (a) Well-to-seismic tie using a deterministic wavelet estimation and a correction on the entire density log. The correlation improved from 0.71 to 0.75 when performing the correction. (b) Well-to-seismic tie using a deterministic wavelet estimation and a correction on the density log only where the caliper indicates a severe borehole enlargement. The correlation improved from 0.71 to 0.77 when performing the correction.

Figures 6 and 7 show the results of the well-to-seismic tie for the CMP 809 of the Viking Graben field, with and without the correction on the density log. The results are divided into three sections: (1) well-to-seismic tie using a statistical wavelet estimation and a correction on the density log only where the caliper indicates a severe borehole enlargement, (2) well-to-seismic tie using a deterministic wavelet estimation and a correction on the entire density log, and (3) well-to-seismic tie using a deterministic wavelet estimation and a correction on the density log only where the caliper indicates a severe borehole enlargement.

The results show that for the three cases, the correlation improved after the correction. The best improvement was achieved for the statistical case: an increase of 7% on the correlation between the real and synthetic seismic traces. In this case, because the statistical estimation of the wavelet through the predictive deconvolution does not require the reflectivity series as an input, the same wavelet is used for the original well-to-seismic tie and the corrected well-to-seismic tie. The wavelet was estimated by the predictive deconvolution of the segment from 1.38 to 1.6 s of the real seismic trace, using the optimum parameters returned by the semiautomatic algorithm (Macedo et al., 2017), with a prediction lag $\alpha = 13$ and filter length $N = 14$.

The well-to-seismic tie using the deterministic estimation of the wavelet show that the best correlation was achieved when the correction on the density log is performed only on the segment where the caliper indicates a severe borehole enlargement and the rest of the density log remains as the original, with an improvement of 6% on the correlation between the real and the synthetic seismic traces. As in this case, a different density log (because of the correction) results in different reflectivity series, and the deterministic estimation of the wavelet requires the reflectivity series as an input, wherein different wavelets are extracted. The wavelets used for the deterministic case are shown in Figure 8.

Although the density of the drilling mud is a known factor during the completion of the well, and its density varies

according to the conditions of the borehole, we analyzed how the ρ_{mud} affects the correlation between the real and synthetic seismic traces after the correction on the density log. We used a range from $\rho_{mud} = 1.10$ g/cm^3 to $\rho_{mud} = 1.30$ g/cm^3 to contemplate the typical values for the density of the drilling mud. The results are shown in Figure 9.

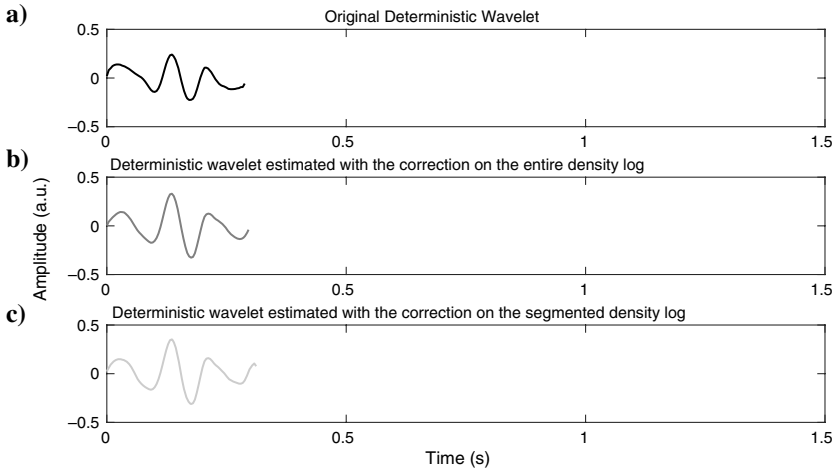

Figure 8. The extracted deterministic wavelets used on the well-to-seismic tie in Figure 7. (a) The original wavelet. (b) The wavelet used in the case of correction on the entire density log. (c) The wavelet used in the case of correction on the segment where the caliper is unstable.

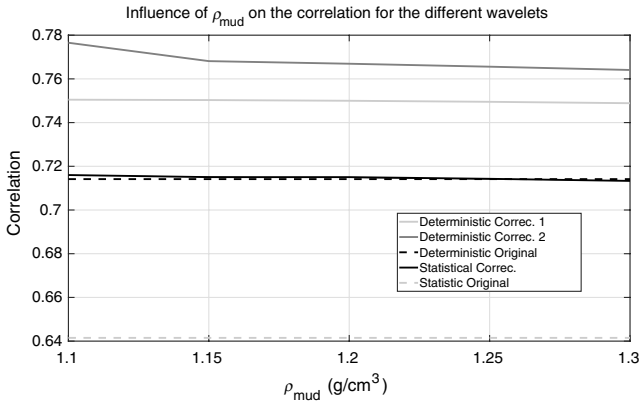

Figure 9. The influence of ρ_{mud} on the correlation between the real and synthetic seismic traces. Deterministic correction 1 (solid light-gray line) indicates the correlation for the case in which the correction is made on the entire density log using the deterministic wavelet; deterministic correction 2 (the solid dark-gray line) indicates the correlation for the case where the correction is made on the segment where the caliper is unstable using the deterministic wavelet; the deterministic original (dashed black line) indicates the original correlation of the well-to-seismic tie when no corrections are made using the deterministic wavelet; statistic correction (the solid black line) indicates the correlation for the case in which the correction is made on the segment where the caliper is unstable using the statistical wavelet; statistic original (the dashed light gray line) indicates the original correlation of the well-to-seismic tie when no corrections are made using the statistical wavelet.

It is observed that the greatest influence of ρ_{mud} on the well-to-seismic tie was for the case where a correction on the anomalous segment of the caliper log is made, and using the deterministic wavelet, where a change from $\rho_{mud} = 1.10$ g/cm^3 to $\rho_{mud} = 1.30$ g/cm^3, causes the correlation between dropping approximately 1.5%. For all of the other cases, the change in ρ_{mud} causes a change of less than 1% on the correlation between the real and synthetic seismic traces.

Conclusion

We have proposed a method to correct the density log for the borehole enlargement at each point in depth using Doll's geometric factor theory to obtain a more accurate well-to-seismic tie for the real data set from the Viking Graben, North Sea. The first step is to set the minimum and maximum values of G_{mud} and associate them to the caliper readings to generate the G_{mud} profile according to prior information and the depth of investigation of the logging tool. The G_{mud} log represents the geometric factor relative to the density of the drilling mud that interacts with the formation on the washout zones. This procedure makes it possible to associate the geometric factor of the mud with the segments in which there is enlargement of the borehole diameter. Those specific areas have their density log corrected, and we then performed the well-to-seismic tie. We estimate the seismic wavelet through a statistical and a deterministic approach: For the statistical case through the predictive deconvolution, only the seismic trace is used, whereas for the deterministic case, the seismic trace and the reflectivity — calculated with the corrected density log — are used. Our analysis agrees with previously published works that an anomalous segment of caliper contributes to lower the correlation on the well-to-seismic tie. The results showed that both ties had their correlations increased with the correction on the density log.

However, it is recommended to test different values for the maximum G_{mud} according to the depth of investigation of the logging tool: It is necessary to establish a higher weight for the physical property that the logging tool has the lowest sensitivity. Because the density logging tool is more sensitive to the near-borehole zones, it is recommended that the geometric factor of the formation far from the borehole be higher than the weight of the washout zone to avoid unrealistic densities values. The limiting assumptions of this methodology is that the geometric factor G varies linearly with the mudcake thickness and that it does not depend on formation properties.

For further work, it is worthwhile to apply this methodology of correction on density log on another data set

that also has an anomalous caliper due to severe enlargement of the borehole. Moreover, we also suggest verifying how this methodology behaves with different methods of wavelet estimation on the well-to-seismic tie, especially the ones that do not imply a minimum-phase wavelet. A comparison of this approach of correction with the traditional spine-rib plot is also recommended, as well as a deeper study of how to circumvent the limitations of this methodology.

Acknowledgments

The authors would like to thank Exxon Mobil for providing the Viking Graben data set. This work was kindly supported by the Brazilian agencies INCT-GP and CNPq and the Geophysics Graduate Program at the Federal University of Pará. We would also like to thank the reviewers and editor for the useful suggestions and corrections.

Data and materials availability

Data associated with this research are available and can be accessed via the following URL: Note: A digital object identifier (DOI) linking to the data in a general or discipline-specific data repository is strongly preferred.

References

Buland, A., and H. Omre, 2003, Bayesian wavelet estimation from seismic and well data: Geophysics, **68**, 2000–2009, doi: 10.1190/1.1635053.

Chok, N. S., 2010, Pearson's versus Spearman's and Kendall's correlation coefficients for continuous data: Ph.D. thesis, University of Pittsburgh.

Doll, H. G., 1949, Introduction to induction logging and application to logging of wells drilled with oil base mud: Journal of Petroleum Technology, **1**, 148–162, doi: 10.2118/949148-G.

Ellis, D. V., and J. M. Singer, 2007, Well logging for earth scientists, 2nd ed.: Springer.

Hauke, J., and T. Kossowski, 2011, Comparison of values of Pearson's and Spearman's correlation coefficients on the same sets of data: Quaestiones Geographicae, **30**, 87–93, doi: 10.2478/v10117-011-0021-1.

Keys, R. G., and D. J. Foster, 1998, Comparison of seismic inversion methods on a single real data set, open file publications: SEG.

Labo, J., 1987, A practical introduction to borehole geophysics: An overview of wireline well logging principles for geophysicists: SEG, Density Log Principles 8.

Liu, Z., and J. Zhao, 2015, Correcting hole enlargement impacts on density logs for coalbed methane reservoirs: The Open Petroleum Engineering Journal, **8**, 72–77, doi: 10.2174/1874834101508010072.

Lundsgaard, A. K., H. Klemm, and A. J. Cherrett, 2015, Joint Bayesian wavelet and well-path estimation in the impedance domain: Geophysics, **80**, no. 2, M15–M31, doi: 10.1190/geo2014-0378.1.

Macedo, I. A. S., C. B. da Silva, J. de Figueiredoa, and B. Omoboyac, 2017, Comparison between deterministic and statistical wavelet estimation methods through predictive deconvolution: Seismic to well tie example from the North Sea: Journal of Applied Geophysics, **136**, 298–314, doi: 10.1016/j.jappgeo.2016.11.003.

Madiba, G. B., and G. A. McMechan, 2003, Processing, inversion, and interpretation of a 2D seismic data set from the North Viking Graben, North Sea: Geophysics, **68**, 837–848, doi: 10.1190/1.1581036.

Oldenburg, D., S. Levy, and K. Whittal, 1981, Wavelet estimation and deconvolution: Geophysics, **46**, 1528–1542, doi: 10.1190/1.1441159.

Robinson, E. A., and S. Treitel, 2008, Digital imaging and deconvolution: The ABCs of seismic exploration and processing: SEG.

Serra, O., 1994, Fundamentals of well logging interpretation — 1. The acquisition of logging data: Elsevier, Development in Petroleum Science 15A.

White, R., and R. Simm, 2003, Tutorial: Good practice in well ties: First Break, **21**, 75–83.

White, R. E., and T. Hu, 1998, How accurate a well tie can be?: The Leading Edge, **17**, 1065–1071, doi: 10.1190/1.1438091.

Yilmaz, O., 2000, Seismic data analysis: Processing, inversion, and interpretation of seismic data: SEG.

Yong, S. H., and C. M. Zhang, 2007, Logging data processing and interpretation: Petroleum University Press, 59–61.

Isadora A. S. de Macedo received a B.S. (2014) from the Federal University of Pará (UFPA) with a year abroad at the University of California - Riverside (UCR); a M.S. (2015) and a Ph.D. (2019) in geophysics from the Federal University of Pará (UFPA). Currently, she is a postdoc researcher in geophysics also at the UFPA. She is a member of SEG and SBGf-Brazil. Her research interests include geophysical modeling and inversion (particularly seismic and electromagnetic methods), petrophysics, and well-to-seismic-tie.

José Jadsom S. de Figueiredo received a B.S. (2006) in physics from the Federal University of Paraiba (UFPB), an M.S. (2008) in physics, and a Ph.D. (2012) in petroleum science and engineering from the State University of Campinas (UNICAMP). While working toward his Ph.D., he spent one year at Allied Geophysical Laboratories at the University of Houston. In October 2012, he joined the Faculty of Geophysics at the Federal University of Pará as a permanent professor. He is a member of SEG, EAGE, and SBGfBrazil. His research interests include seismic imaging methods (particularly

diffraction imaging), physical modeling of seismic phenomena, anisotropy, rock physics, petrophysics, and well ties.

Matias Costa de Sousa received a B.S. (2017) and a master's degree (2019) in geophysics from UFPA. He is currently a Ph.D. student of the Postgraduate Programme in Geophysics (CPGf), where he studies methodologies of correlating seismic and well-log data, especially for geopressure analysis. His research interests include seismic imaging, electromagnetic methods, borehole geophysics, and rock physics.